ISSN 2816-8089

RESEARCH ARTICLE

Identification of Antibiotic Drugs against SARS-CoV2 Mpro: A Computational Approach for Drug Repurposing

Hridoy R. Bairagya[1*], Sweety Gupta[2], Sayanti Pal[1]

[1]*Computational Drug Design and Bio-molecular Simulation Lab, Department of Bioinformatics, Maulana Abul Kalam Azad University of Technology, Haringhata, 741249, West Bengal, India.*
[2]*Department of Pharmaceutical Technology, Maulana Abul Kalam Azad University of Technology, Haringhata, 741249, West Bengal, India.*

Abstract

The coronavirus pandemic has posed a significant challenge for researchers seeking to develop new compounds and repurpose existing drugs to manage this disease. It has been found that the Main protease enzyme (Mpro) is critical to the replication of the virus, making it an attractive target for drug development. Different antibiotics have been proven effective against different viruses, leading to their recommendation for COVID-19.

In this study, virtual screening, pharmacokinetics, QSAR, and molecular docking techniques were used to investigate the best antibiotic drugs for COVID-19 by targeting the active and inactive conformations of the Mpro enzyme. The results of the study demonstrate that Praziquantel is a promising candidate for COVID-19 treatment. This is due to several reasons: First, Praziquantel exhibits better binding energy in both the conformations of Mpro. Second, it binds in S-3A site in native conformation and S-1B in active state. Third, Praziquantel has excellent absorption properties, strong blood-brain barrier penetration power, and reasonably good solubility.

Therefore, the study nominates Praziquantel as the best option for future experimental and pre-clinical investigations for COVID-19.

Key Words: *SARS-CoV-2 Mpro; Clarithromycin; Levofloxacin; Oseltamivir structural analogues; Molecular docking*

***Corresponding Author**: Hridoy R. Bairagya, Associate Professor, Computational Drug Design and Bio-molecular Simulation Lab, Department of Bioinformatics, Maulana Abul Kalam Azad University of Technology, West Bengal, India; Email: hbairagya@gmail.com*

***Received Date**: December 11, 2023, **Accepted Date**: January 30, 2024, **Published Date**: February 08, 2024*

***Citation:** Bairagya HR, Gupta S, Pal S. Identification of Antibiotic Drugs against SARS-CoV 2Mpro: A Computational Approach for Drug Repurposing. Int J Bioinfor Intell Comput. 2024;3(1):70-90.*

Graphical Abstract

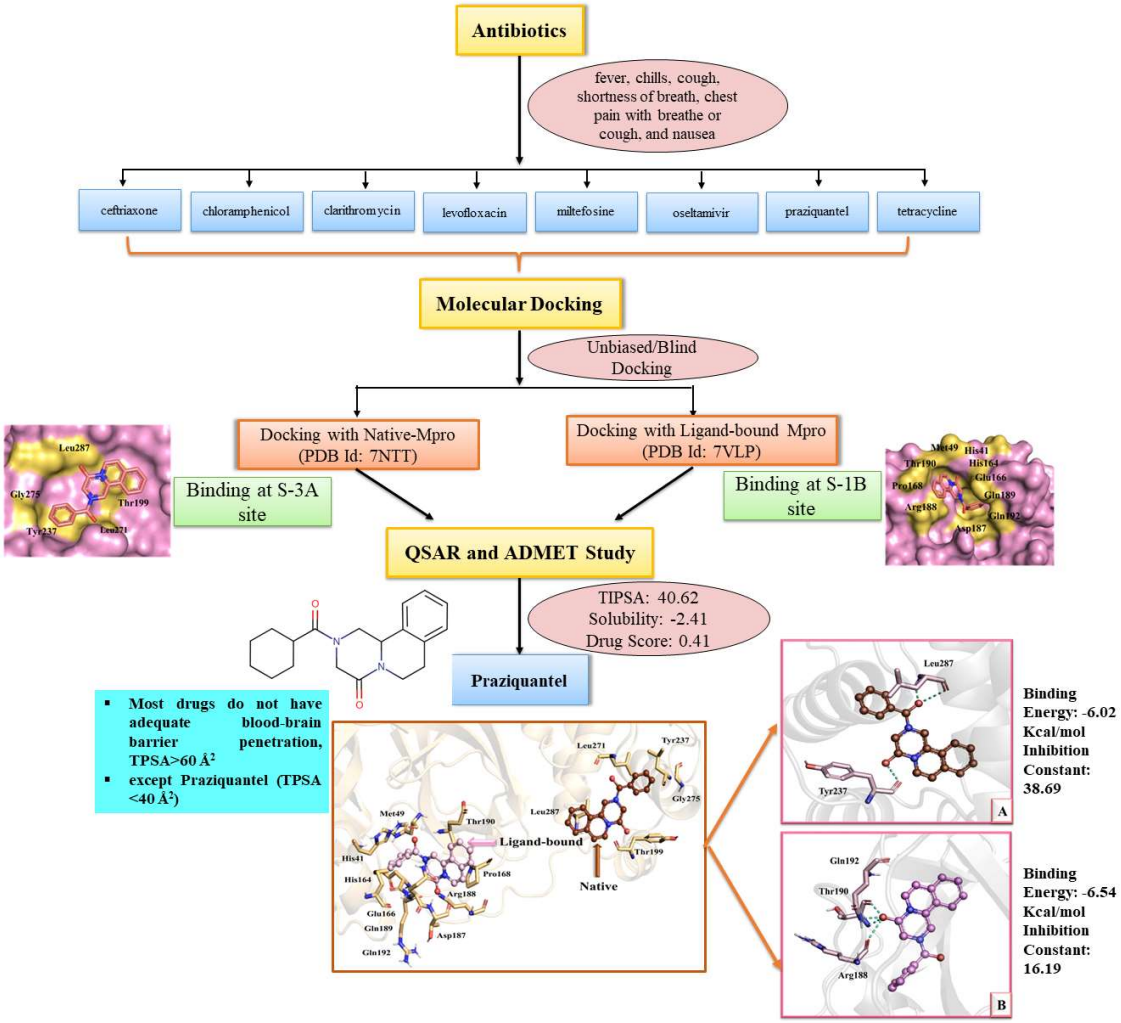

Abbreviations

SARS-CoV-2: Severe Acute Respiratory Syndrome Coronavirus 2; COVID-19: Coronavirus disease 2019; Mpro: Main protease; WHO: World Health Organization; GA: Genetic Algorithms

1. Introduction

On March 11th, 2020, the World Health Organization (WHO) declared a global pandemic for Coronavirus Disease 2019 (COVID-19) due to tremendous societal and economic disruptions [1]. The pandemic resulted in a global health crisis with more than 3.5 million deaths worldwide [2]. Since COVID-19 is a viral disease, treatment with antibiotics is inappropriate but the viral respiratory infections may clinically progress to bacterial pneumonia requiring antibiotic administration. Most of the local guidelines as well as some international guidelines

advocated for the use of antibiotics based on the epidemiology of local pathogens and resistance patterns. The advantage of the use of antibiotics is that they cover most of the opportunistic pathogens that could cause secondary infection in COVID-19 [3]. No drugs have been approved for the treatment of severe COVID-19 infections to date. However, besides vaccine development, the recent demands are an essential call for the discovery of new potential anti-COVID molecules for severe COVID-19 treatment.

Several antibiotics such as azithromycin, doxycycline, clarithromycin, ceftriaxone, amoxicillin, amoxicillin-clavulanic acid, ampicillin, gentamicin, erythromycin, benzylpenicillin, piperacillin/tazobactam, ciprofloxacin, ceftazidime, cefepime, vancomycin, meropenem, and cefuroxime were recommended by the doctor and were used in the management of COVID-19, starting from asymptomatic, mild, moderate, and severe COVID-19 with or without complications [4]. In a study, 71% of the hospitalized COVID-19 patients received antibiotics despite a confirmed bacterial co-infection rate of only 1% [5] and a systematic review showed the mean rate of antibiotic use was 74% [6]. However, the increased use of antibiotics has become challenging especially for low and middle-income countries due to the lack of proper infrastructure in health care service. Seventeen different antibiotic drugs belonging to seven antibiotic classes were used to manage the health crises during the pandemic [3,7]. The common antibiotics in use for patients were ceftriaxone (54.00% of patient), vancomycin (48.00% of patient), azithromycin (47.00% of patient)), and cefepime (45.00% of patient) [8]. Ceftriaxone (73.08% patient) and azithromycin (52.88% of patient) were widely used antibiotics used in the management of COVID-19 patients [3]. Fluoroquinolones were most used for patients (56.80%), followed by ceftriaxone (39.50%), then azithromycin (29.10%) [3], and carbapenems were also administered and used in up to 40.10% of patients [6]. Among the third-generation antibiotics, ceftriaxone and Moxifloxacin were used but doxycycline or other tetracycline group of drugs was not administered during the COVID-19 management.

The Main protease (Mpro) of severe acute respiratory syndrome coronavirus 2 (SARS-CoV-2) is a crucial enzyme of Coronaviruses and has a pivotal role in mediating viral replication and transcription and making it as an attractive drug target for SARS-CoV-2 [9]. The monomer of Mpro is enzymatically less active and its hydrolytic activity is seen in its dimeric form, which serves as a functional unit with two 306-residue long [10]. The Mpro contains three domains, domain I (residues 8–101) and domain II (residues 102–184) have an antiparallel β-barrel structure. Domain III (residues 201–303) contains five α-helices arranged into a largely antiparallel globular cluster, and it is connected to domain II by a long loop region (residues 185–200). A catalytic dyad transfers a single proton from Cys145 to His41. At the same time, Cys145's sulfur atom engages in a nucleophilic attack on the carbonyl carbon of the peptide bond to produce an intermediate known as thio-hemiketal. The active site of this enzyme comprises a catalytic dyad His41 and Cys145, and lacks the third catalytic residues, while one water molecule takes the responsibility of third partner, also act as catalytic machinery system and is stabilized by His164. Possibly, this water is energetically favorable (or has the potentiality) and may contain reasonable entropy to activate the zwitter catalytic dyad Cys–145–His+41 residues [11].

The vision of the present study is to investigate and identify the best antibiotic drugs against Main proteases (Mpro). Few computational studies shed light on the anti-biotic drugs for Mpro protein by several research groups [12-14]. Our previous investigation highlights that azithromycin is the best antibiotic drug rather than remdesivir, lopinavir, and their analogs

erythromycin, sofosbuvir and 3-Amino-N-{4-[2-(2,6-Dimethyl-Phenoxy)-Acetylamino]-3-Hydroxy-1-Isobutyl-5 Phenyl-Pentyl}-Benzamide respectively [14]. However, the present computational study focused on eight antibacterial drugs ceftriaxone, chloramphenicol, clarithromycin, levofloxacin, miltefosine, oseltamivir, praziquantel, and tetracycline excluding other drugs because there are several viruses that can cause common colds, making it difficult to determine if someone has COVID-19 or another viral illness without proper testing. For this reason, some doctors prefer to prescribe antibiotics to patients with acute cough or lower respiratory tract infections to help them recover and avoid hospitalization. It is believed that these antibiotics may play an important role in the treatment of COVID-19 and are therefore included in this study.

Ceftriaxone is a third-generation antibacterial drug that can be administered both intravenously and intramuscularly during the treatment of lower respiratory tract infections [15]. Chloramphenicol is a broad-spectrum antimicrobial agent that acts on plastic anemia and bone marrow suppression in humans [16]. Clarithromycin is an oral macrolide that was approved by the FDA in 1991 for the treatment of respiratory infections [17]. Levofloxacin is the L-form of the fluoroquinolone antibacterial agent of loxacin and it demonstrated a broad range of activity against Gram-positive and-negative organisms and anaerobes [18]. Miltefosine is an alkylphosphocholine that has been approved recently for the treatment of visceral leishmaniasisand it also used for paracoccidioidomycosis [19]. During the ongoing outbreak of coronavirus disease 2019 (COVID-19), most patients with COVID-19 who are symptomatic have used oseltamivir [20]. Praziquantel was developed in the 1970s and it is the only drug for the treatment of human schistosomiases, due to high efficacy, excellent tolerability, few and transient side effects, simple administration, and competitive cost [21]. Tetracyclines possess many properties considered ideal for antibiotic drugs, including activity against Gram-positive and-negative pathogens, proven clinical safety, acceptable tolerability, and the availability of intravenous [22].

It has been found that the use of antibiotics and steroids for treating COVID-19 has fewer side effects when compared to standard care. Lab tests and computer simulations have also shown that antibiotics and steroids can inhibit a key enzyme used by SARS-CoV-2. The in-vitro antiviral activity of doxycycline against a clinical isolate of SARS-CoV-2 has also shown promise, as it is effective at both the entry and post-entry stages of the virus. The computer-aided drug design method developed the mechanism-based inhibitor (N3), and determining its crystal structure with Mpro of SARS-CoV-2 is a promising *in silico* approach that justifies its usage in practical utility.

Multiple analyses of crystal structures of the inactive and active form of Mpro protein revealed which conformation will be considered for further investigation. Thus, this is another computational report from our research groups that explores molecular docking results on the two alternative conformations of catalytic His41 of the Mpro enzyme. Moreover, an *in silico* study of the absorption, distribution, metabolism, and excretion (ADME) properties of the all antibiotic drugs were performed by investigating their match of Lipinski's rules, topological polar surface area (TPSA) and percentage of absorption (%ABS). Computational ADME test is currently used widely to determine whether it is possible for a drug candidate to reach its site of action. No computational study has yet been reported on the above mentioned eight anti-biotic drugs with two alternative conformations of Mpro protein. The recent computational investigation acts as a complementary approach for repurposing of anti-biotic drugs and evaluate the existing them for COVID-19 disease.

2. Materials and Methods

2.1. Structure collection

The thirty crystal structures of SARS-CoV-2 Main Protease (Mpro) were obtained from the RCSB database [23] with dimeric conformation to choose the best receptor for molecular docking study. On the basis of Mpro conformation, the two criteria were adopted for receptor selection; (i) native and (ii) ligand-bound. The PDB Id. 7NTT (resolution 1.74 Å) is the native form of Mpro where ND1 of His41 faces towards the surface of ligand binding pocket whereas in contrast, the above-mentioned atom gets reverse direction and occupies towards the inner site of pocket.

2.2. Investigation of antibacterial drugs for virtual screening study

The SMILES and 3D conformations of eight antibacterial drugs like Ceftriaxone (DB01212), Chloramphenicol (DB00446), Clarithromycin (DB01211), Levofloxacin (DB01137), Miltefosine (DB09031), Oseltamivir (DB00198), Praziquantel (DB01058), and Tetracycline (DB00759) were obtained from the Drug-Bank (v5.1.5) [24], for the molecular docking study with the two receptors (PDB Id. 7NTT and 7VLP).

The Osiris property explorer [25] and Swiss-ADME [26] programs have been used to compare the pharmacokinetics and drug-likeness scores between Ceftriaxone, Chloramphenicol, Clarithromycin, Levofloxacin, Miltefosine, Oseltamivir, Praziquantel, and Tetracycline. Each molecule was screened based on six molecular properties (cLogP, solubility, molecular weight, TPSA, drug-likeness, and drug score) from the Osiris program three characters (Lipinski, bioavailability score, and synthetic accessibility) from Swiss-ADME program.

2.3. Molecular docking

2.3.1. Receptor and ligand preparation

Two conformations of receptor Mpro and eight ligands were prepared usingAutoDockTools (ADT, v1.5.6) [27]. The native (PDB Id. 7NTT) and ligand-bound (PDB Id. 7VLP) crystal structures were taken as the receptors. Furthermore, ligands, water molecules, and heteroatoms were removed from two crystal structures. Then polar hydrogen bonds, AD4-type atoms, and Gasteiger charges were incorporated into each receptor Mpro. The Kollman-united charge was used to calculate the partial atomic charge of each ligand and torsional angles with rotatable bonds of each ligand are assigned accordingly.

2.3.2. Molecular docking

The molecular docking was employed using AutoDockTools 1.5.7 and Autodock 4.0 program [28-30] for grid generation and molecular docking, respectively. The conformations of two receptors were kept fixed (rigid), and all the ligands were prepared as flexible with appropriate assignment of their rotatable bonds. The blind molecular docking study was followed by two consecutive methods; category-I with native conformation (PDB Id. 7NTT) and category-II accompanied by ligand-bound form (PDB Id. 7VLP) was considered. Affinity maps for all the present atom types and an electrostatic map were computed with a grid

spacing of 0.97 Å in 7NTT and 7VLP. Consequently, the Genetic Algorithms (GA) was performed for 100 steps based on its binding energy. Then, the structural models were collected from the lowest energy docking results.

3. Results and Discussion

3.1. Analysis of the Mpro-crystal structures

The nine crystal structures of native and twenty-one ligand-bound dimeric conformations of Mpro proteins were obtained from the Protein Data Bank. Several research groups have independently solved these structures using PHENIX, REFMAC, and BUSTER refinement programs at different (4.6–8.5)pH. The crystallographic structural parameters (c.s.p.) such as Matthews coefficient, solvent content, and calculated mean B-factors of protein are found maximum in 7VK3 and 7VK4 of native and 7VLQ in ligand-bound conformation. Moreover, the observed ratio of the number of protein atoms concerning water molecules (NPROT/NHOH) in Mpro-native and ligand-bound form are different ranges that suggest 7VK7 of native and 7NT1 of the ligand-bound ensemble are random compared to remaining structures. Most dimer native-Mpro crystal structures belong to space group P 1 21 1, whereas ligand-bound structures are from P 21 21 21 or P 1 21 1. The native structure has been observed to have over 52,000 reflections, while the ligand-bound structure has been found to have over 76,000 (Table S1 and S2.) Therefore, 7NTT of native and 7VLP of ligand-bound form were considered as reference structures for the present computational study.

3.2. Binding pose analysis of antibiotic drugs

Computational molecular docking studies are effective tools broadly utilized to interpret the molecular aspects of ligand–protein interactions during drug discovery against COVID-19 disease. Our computational drug repurposing workflow against Mpro-native and ligand-bound forms was started with a molecular docking study of five FDA-approved drugs and one new ligand.

In this approach, we have elucidated how the antibiotics bind and interact with the native and ligand-bound form of Mpro. The docking methods were used in blind mode, meaning that no reference ligand was considered. As a result, the RMSD value of docked ligands was not taken into account for further studies. In blind docking, it's necessary to identify the target pocket without any prior knowledge or predefined binding sites. Therefore, the binding pose of each antibiotic drug at the Mpro receptor has been analyzed based on the binding energy of the ligands, which can be found in Table 1. The drug molecule Chloramphenicol binds in the domain DI, Oseltamivirin the DI-DII interface, Ceftriaxone in the DII, Clarithromycin in the DII-DIII interface and the remaining drug molecules (Levofloxacin, Miltefosine, Praziquantel, and Tetracycline) in domain DIII in the native conformation Figure 1. Consequently, in a ligand-bound state, the molecules Chloramphenicol, Miltefosine, Oseltamivir, Praziquantel, and Tetracycline are observed to bind at domain DI-DII interface region, Ceftriaxone in domain DII - DIII interface, and Clarithromycin and Levofloxacin in DIII domain Figure 2. The four antibiotic drugs bind at the DIII domain in native conformation and five at the DI-DII interface in the ligand-bound state in the Mpro protein. Hence, the above-mentioned computational results suggest the domain DIII in native conformation and DI -DII interface

region for ligand-bound form is energetically preferable for binding most of the antibiotic drugs in the Mpro protein.

Table 1: *Comparative analysis of the docking results between native (PDB Id: 7NTT) and ligand-bound Mpro (PDB Id: 7VLP).*

Antibiotics	Category-I (Native)		Category-II (Ligand-bound)	
	Binding Energy (kcal/mol)	Inhibition Constant (Ki)	Binding Energy (kcal/mol)	Inhibition Constant (Ki)
Ceftriaxone	-5.54	86.38 uM	-5.69	67.84 uM
Chloramphenicol	-5.19	156.30 uM	-5.64	73.88 uM
Clarithromycin	-8.56	530.74 nM	-8.81	347.82 nM
Levofloxacin	-5.13	174.43 uM	-5.40	110.28 uM
Miltefosine	-4.84	283.53 uM	-6.09	34.41 uM
Oseltamivir	-4.29	720.45 uM	-5.12	175.21 uM
Praziquantel	-6.02	38.96 uM	-6.54	16.19 uM
Tetracycline	-7.44	3.55 uM	-8.19	995.60 nM

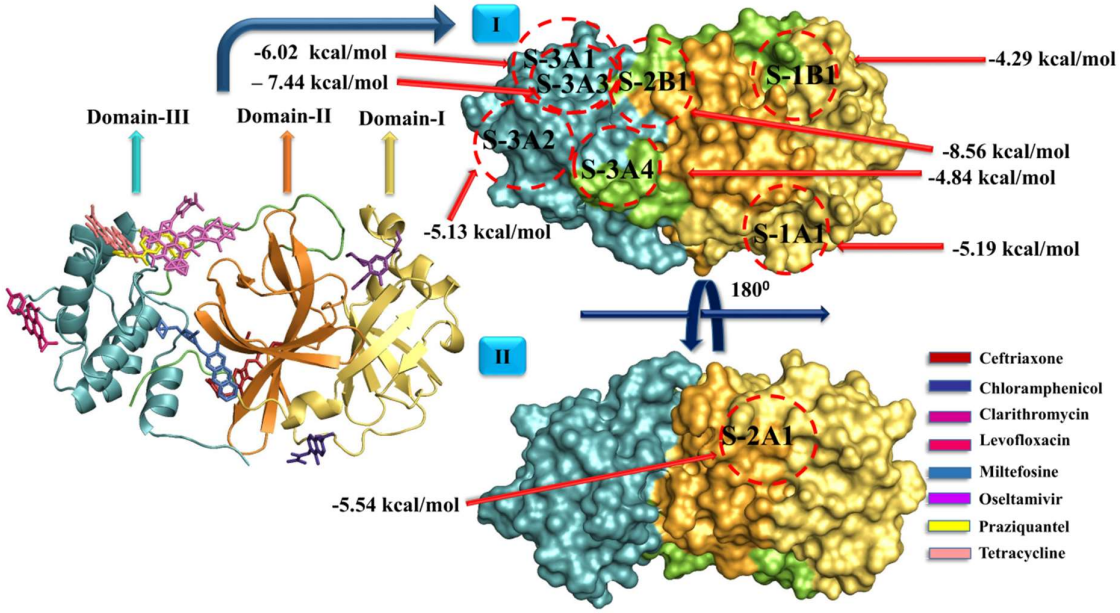

Figure 1: *Unbiased docking of eight antibacterial drugs (Ceftriaxone, Chloramphenicol, Clarithromycin, Levofloxacin, Miltefosine, Oseltamivir, Praziquantel, Tetracycline) with native Mpro*

(PDB Id: 7NTT); Representation of binding zone of ligands as domain DI: S-1A (sub-category: S-1A1), DI and DII intersect: S-1B (sub-category: S-1B1), DII: S-2A (Sub-category: S-2A1) , DII and DIII intersect: S-2B (sub-category: S-2B1), DIII: S-3A (sub-category: S-3A1, S-3A2, S-3A3, S-3A4); Category-I represents the binding zone of ligands, shown as S-1A1, S-1B1, S-2B1, S-3A1, S-3A2, S-3A3 and S-3A4; Category-II represents binding zone at 180⁰ rotation of the crystal structure shown as S-2A1.

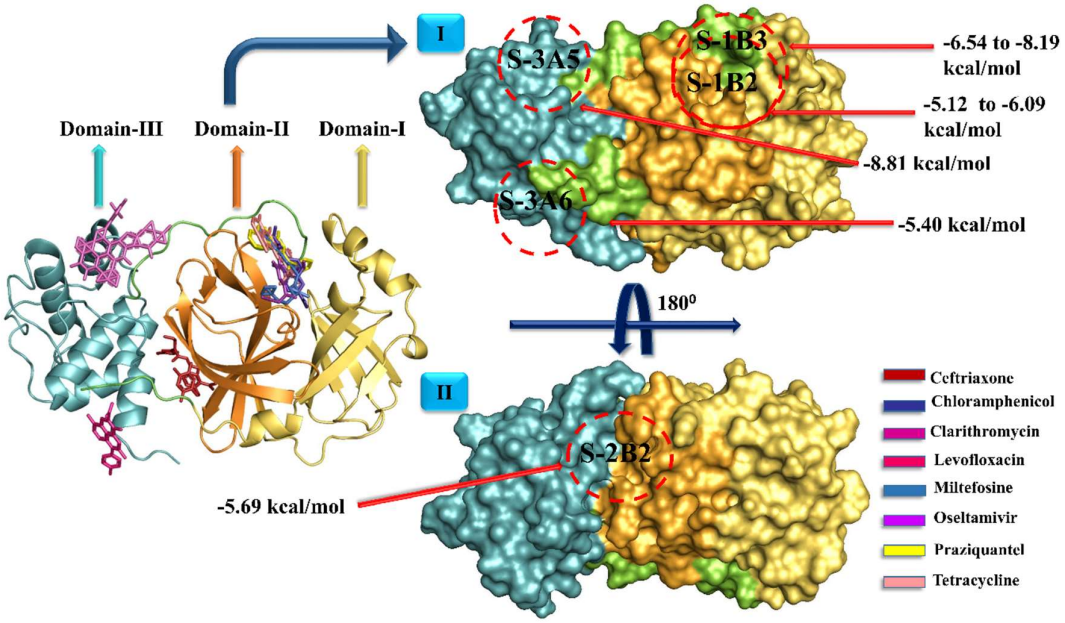

Figure 2: *Unbiased docking of eight antibacterial drugs (Ceftriaxone, Chloramphenicol, Clarithromycin, Levofloxacin, Miltefosine, Oseltamivir, Praziquantel, Tetracycline) with ligand-bound Mpro (PDB Id: 7VLP); Representation of binding zone of ligands as domain DI and DII intersect: S-1B (sub-category: S-1B2, S-1B3), DII and DIII intersect: S-2B (sub-category: S-2B2), DIII: S-3A (sub-category: S-3A5, S-3A6); Category-I represents the binding zone of ligands, shown as S-1B2, S-1B3, S-3A5, S-3A6; Category-II represents binding zone at 180⁰ rotation of the crystal structure shown as S-2B2.*

In detail, the binding zones of all antibiotic drugs were categorized as S-1A, S-1B, S-2A, S-2B and S-3A and subcategorized as S-1A1, S-1B1, S-1B2, S-1B3, S-2A1, S-2B1, S-2B2, S-3A1, S-3A2, S-3A3, S-3A4,S-3A5 and S-3A6 sub-sites at their respective domains. Domain DI contains sub-site S-1A, DI-DII interface with S-1B, DII with S-2A, DII-DIII with S-2B, and DIII with S-3A. The S-3A site from domain DIII of the native state is energetically favorable for the drug Praziquantel (S-3A1), Levofloxacin (S-3A2), Miltefosine (S-3A4), and Tetracycline (S-3A3), however, its ligand-bound state accepts Clarithromycin drug. Consequently, S-2B sites prefer to bind Clarithromycin (S-2B1) in its native state and Ceftriaxone (S-2B2) in ligand-bound form. Moreover, S-1B is occupied by Oseltamivir (S-1B1) in its native state and also by Chloramphenicol (S-1B2), Miltefosine (S-1B2), Oseltamivir(S-1B2),Praziquantel(S-1B3), and Tetracycline (S-1B3) in ligand-bound form Table 2. Interestingly, the S-1A1 sub-site has a special inclination for binding toward the Chloramphenicol drug, this site is only evolving in the native state but is unavailable in the ligand-bound state. The present computational study highlights S-3A site in its native state and S-1B in ligand bound state of Mpro are structurally more efficient in capturing the anti-biotic drugs.

To investigate the comparative analysis of the binding zone of each antibiotic drug between the ligand-bound and native forms, the superimposed complex structures were analyzed properly. Interestingly, Ceftriaxone partially shares the common binding sites in both conformations of Mpro (Figure 3). The complex conformation revealed that the Clarithromycin molecule comprehensibly binds in an almost similar position in the Mpro protein (Figure 4). The remaining drug molecules Chloramphenicol, Levofloxacin, Miltefosine, Oseltamivir, Praziquantel, and Tetracyclin bind different regions in the native and ligand-bound conformation of Mpro Figures 5-10.

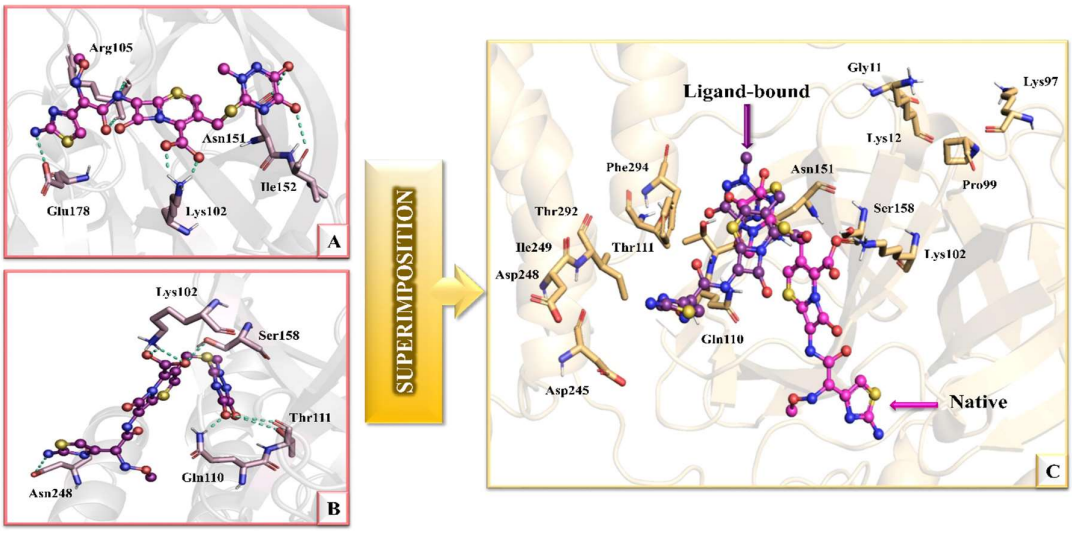

Figure 3: *Comparative analysis of Ceftriaxone with native and ligand-bound Mpro. (A) Ceftriaxone and its neighbouring residues showing Polar interactions during unbiased docking with native Mpro (PDB Id: 7NTT) (B) Ceftriaxone and its neighbouring residues showing Polar interactions during unbiased docking with ligand-bound Mpro (PDB Id: 7VLP) (C) Superimposition of Ceftriaxone with native and ligand-bound Mpro.*

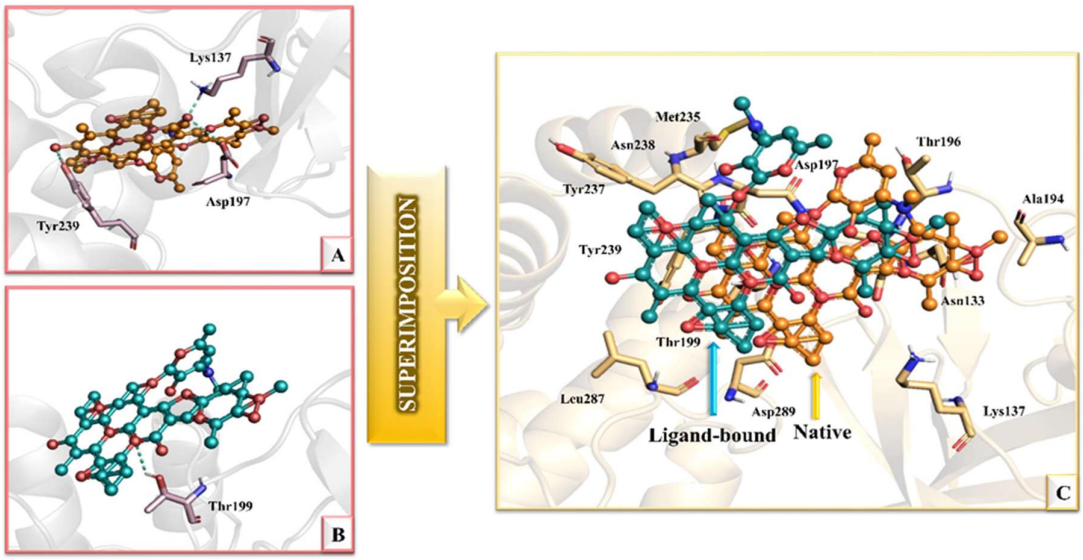

Figure 4: *Comparative analysis of Clarithromycin with native and ligand-bound Mpro. (A) Clarithromycin and its neighbouring residues showing Polar interactions during unbiased docking*

with native Mpro (PDB Id: 7NTT) (B) Clarithromycin and its neighbouring residues showing Polar interactions during unbiased docking with ligand-bound Mpro (PDB Id: 7VLP) (C) Superimposition of Clarithromycin with native and ligand-bound Mpro.

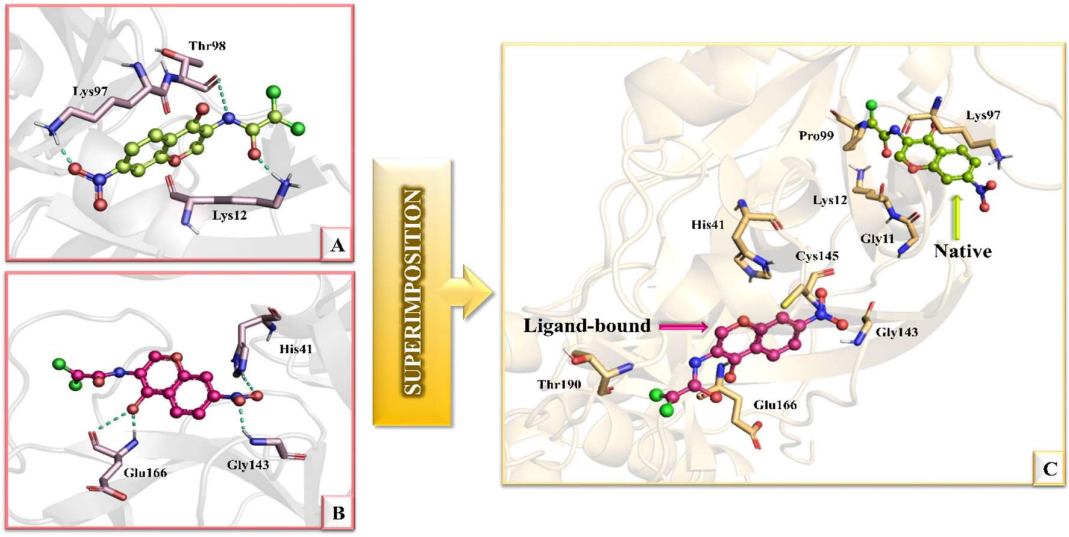

Figure 5: *Comparative analysis of Chloramphenicol with native and ligand-bound Mpro. (A) Chloramphenicol and its neighbouring residues showing Polar interactions during unbiased docking with native Mpro (PDB Id: 7NTT) (B) Chloramphenicol and its neighbouring residues showing Polar interactions during unbiased docking with ligand-bound Mpro (PDB Id: 7VLP) (C) Superimposition of Chloramphenicol with native and ligand-bound Mpro.*

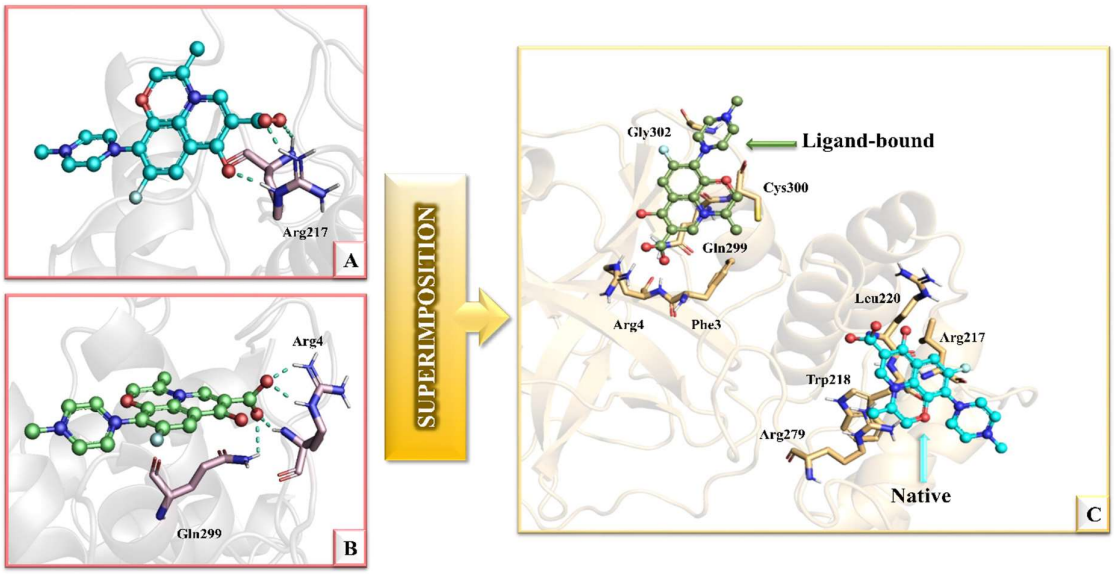

Figure 6: *Comparative analysis of Levofloxacin with native and ligand-bound Mpro. (A) Levofloxacin and its neighbouring residues showing Polar interactions during unbiased docking with native Mpro (PDB Id: 7NTT) (B) Levofloxacin and its neighbouring residues showing Polar interactions during unbiased docking with ligand-bound Mpro (PDB Id: 7VLP) (C) Superimposition of Levofloxacin with native and ligand-bound Mpro.*

Table 2: *Binding zones and corresponding domains for antibacterial drugs.*

Sl. No.	Antibiotics	Category-I (Native)		Category-II (Ligand-bound)	
		Domain (D)/ Structural position	**Residues**	**Domain (D)/ Structural position**	**Residues**
1	Ceftriaxone	D-II S-2A1	Lys102, Arg105, Asn151, Ile152, Glu178	D-II and III S-2B2	Lys102, Gln110, Thr111, Asn151, Ser158, Asp245, Asp248, Ile249, Thr292, Phe294
2	Chloramphenicol	D-I S-1A1	Gly11, Lys12, Lys97, Pro99	D-I and II S-1B2	His41, Gly143, Cys145, Glu166, Thr190
3	Clarithromycin	D-II and III S-2B1	Asn133, Lys137, Ala194, Asp197, Thr199, Tyr237, Asn238, Tyr239, Leu287, Asp289	D-III S-3A5	Thr196, Asp197, Thr199, Met235, Tyr237, Asn238, Tyr239, Leu287
4	Levofloxacin	D-III S-3A2	Arg217, Trp218, Leu220, Arg279	D-III S-3A6	Phe3, Arg4 Gln299, Cys300 Gly302
5	Miltefosine	D-III S-3A4	Arg4, Lys5, Met6, Ala7, Leu282, Ser284, Glu288	D-I and II S-1B2	His41, Leu141 Asn142, Gly143 Ser144, Cys145 His163, Met165 Glu166, Pro168 Thr190
6	Oseltamivir	D-I and II S-1B1	Thr24, Thr25, Thr26, Cys44, Thr45, Ser46, Glu47, Asn142, Gly143, Cys145	D-I and II S-1B2	His41, Leu141, Gly143, Ser144, His163, His164, Met165, Asp187, Gln189
7	Praziquantel	D-III S-3A1	Thr199, Tyr237, Leu271, Gly275, Leu287	D-I and II S-1B3	His41, Met49, His164, Glu166, Pro168, Asp187, Arg188, Gln189, Thr190, Gln192
8	Tetracycline	D-III S-3A3	Tyr237, Tyr239, Leu272, Gln273, Gly275, Met276, Asn277, Gly278, Leu287	D-I and II S-1B3	His41, His164, Met165, Glu166, Pro168, Asp187, Arg188, Thr190, Ala191, Gln192

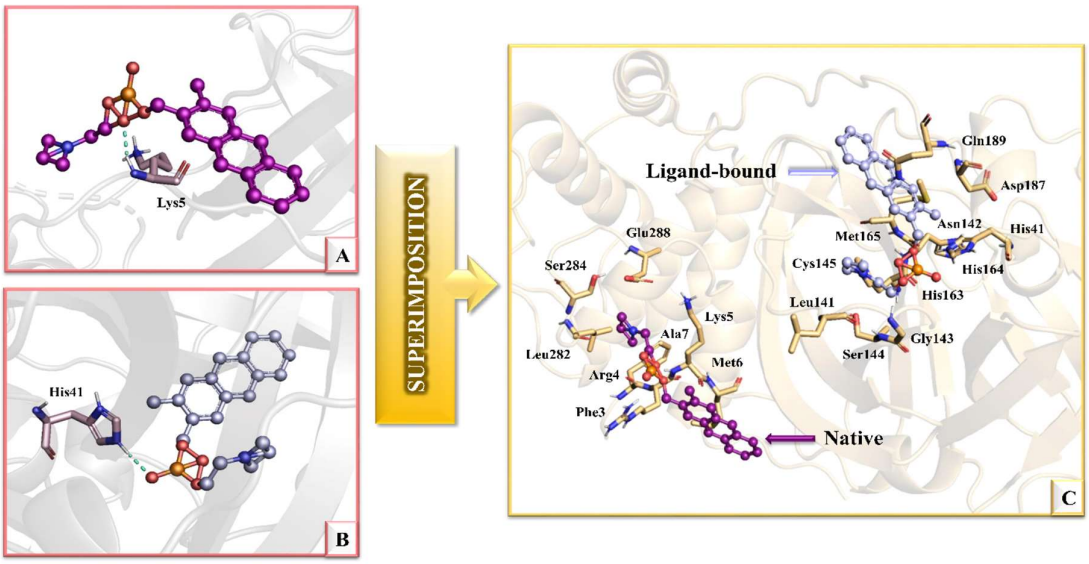

Figure 7: *Comparative analysis of Miltefosine with native and ligand-bound Mpro. (A) Miltefosine and its neighbouring residues showing Polar interactions during unbiased docking with native Mpro (PDB Id: 7NTT) (B) Miltefosine and its neighbouring residues showing Polar interactions during unbiased docking with ligand-bound Mpro (PDB Id: 7VLP) (C) Superimposition of Miltefosine with native and ligand-bound Mpro.*

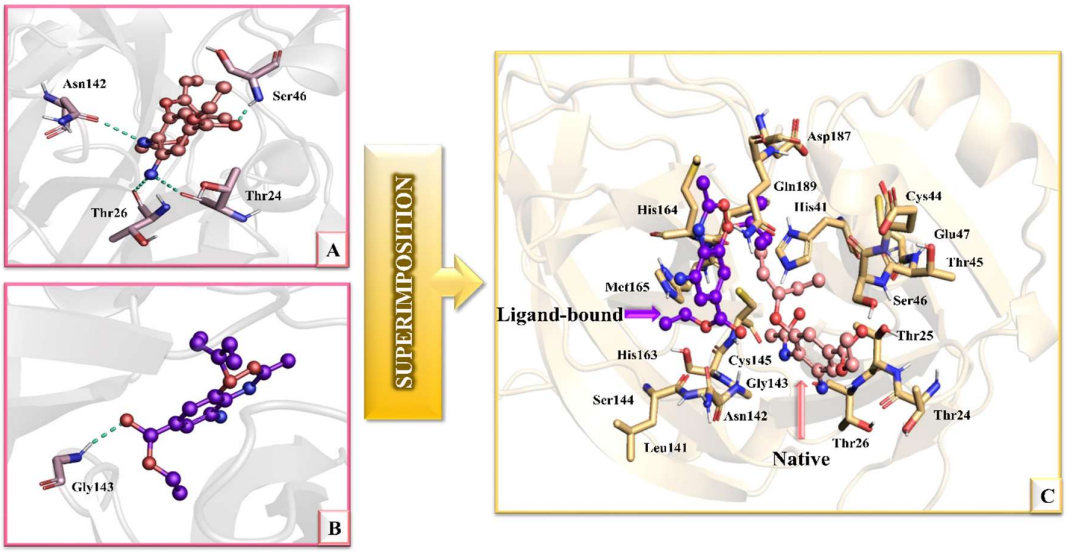

Figure 8: *Comparative analysis of Oseltamivir with native and ligand-bound Mpro. (A) Oseltamivir and its neighbouring residues showing Polar interactions during unbiased docking with native Mpro (PDB Id: 7NTT) (B) Oseltamivir and its neighbouring residues showing Polar interactions during unbiased docking with ligand-bound Mpro (PDB Id: 7VLP) (C) Superimposition of Oseltamivir with native and ligand-bound Mpro.*

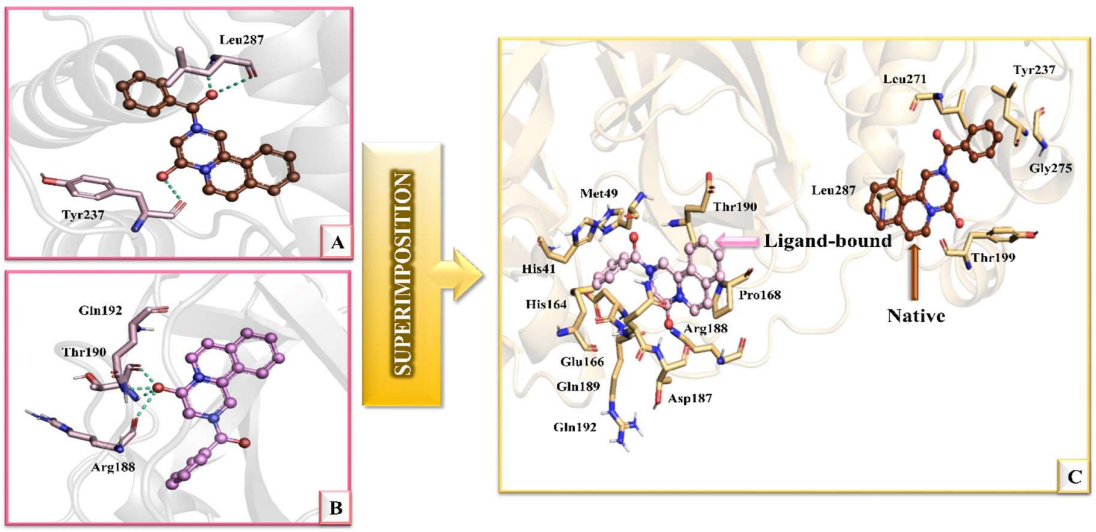

Figure 9: *Comparative analysis of Praziquantel with native and ligand-bound Mpro. (A) Praziquantel and its neighbouring residues showing Polar interactions during unbiased docking with native Mpro (PDB Id: 7NTT) (B) Praziquantel and its neighbouring residues showing Polar interactions during unbiased docking with ligand-bound Mpro (PDB Id: 7VLP) (C) Superimposition of Praziquantel with native and ligand-bound Mpro.*

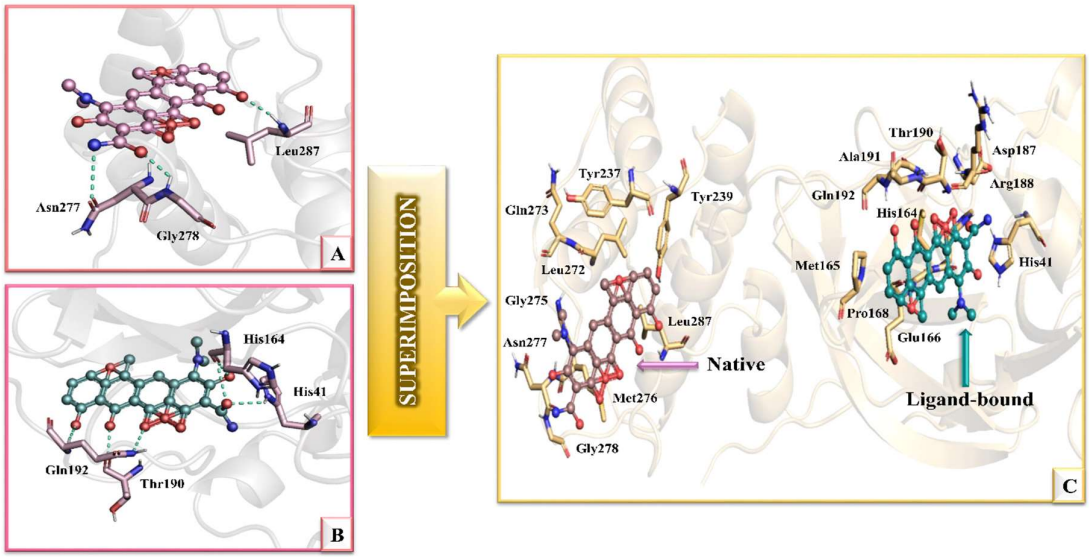

Figure 10: *Comparative analysis of Tetracycline with native and ligand-bound Mpro. (A) Tetracycline and its neighbouring residues showing Polar interactions during unbiased docking with native Mpro (PDB Id: 7NTT) (B) Tetracycline and its neighbouring residues showing Polar interactions during unbiased docking with ligand-bound Mpro (PDB Id: 7VLP) (C) Superimposition of Tetracycline with native and ligand-bound Mpro.*

3.3. Analysis of pharmacokinetics properties and QSAR study

The present study is highly focused on identifying the best anti-biotic drug for COVID disease. Drug-likeness is a promising method to identify a balance that influences the pharmacodynamic and pharmacokinetic properties of some compound that ultimately

optimizes its absorption, distribution, metabolism, and excretion (ADME) in the human body. These parameters were tentatively assessed using theoretical calculations following Lipinski's rule of five, which establishes that the permeation of an orally administered compound is more likely to be efficient. Our results revealed that all drugs have lipophilicities less than 5, with values between -3.01 and 2.54 Table 3. All drugs have a number of hydrogen bond acceptors (HBA) (n-ON=5–9), and their molecular weights were smaller than 500, which is in agreement with Lipinski's rules. Except the Ceftriaxone, Clarithromycin, and Tetracycline they all have a number of hydrogen bond donors (HBD) (n-OHNH=10), violating one of Lipinski's rules.

Table 3: *Pharmacokinetics properties and QSAR study of antibacterial drugs.*

Drugs	cLogP	Solubility	Molecular weight	TIPSA	Drug-Likeness	Drug Score	Lipinski	Bioavailability score	Synthetic accessibility
Ceftriaxone	-3.01	-2.95	554.58	293.80	16.69	0.67	No; 2 violations: MW>500, N or O>10	0.11	5.06
Choramphenicol	-0.42	-2.37	323.13	115.38	-4.61	0.06	Yes; 0 violation	0.55	2.78
Clarithromycin	2.10	-3.77	747.95	182.91	11.06	0.51	No; 2 violations: MW>500, N or O>10	0.17	8.91
Levofloxacin	-0.34	-2.74	361.37	75.01	5.77	0.92	Yes; 0 violation	0.55	3.63
Miltefosine	0.12	-2.39	407.57	68.40	-54.74	0.44	Yes; 0 violation	0.55	5.12
Oseltamivir	0.93	-2.45	312.40	90.65	-1.50	0.56	Yes; 0 violation	0.55	4.44
Praziquantel	2.54	-2.41	312.41	40.62	-0.09	0.41	Yes; 0 violation	0.55	2.90
Tetracycline	-1.33	-1.83	444.43	181.62	5.43	0.83	Yes; 1 violation: NH or OH>5	0.11	5.04

Other rules include the number of rotatable bonds, indicating the flexibility of the molecule, the volume, and the polar surface area. The topological polar surface area (TPSA) is recognized as a good indicator of drug absorption in the intestine (TPSA less than 140 $Å^2$) and blood-brain barrier penetration (TPSA less than 60 $Å^2$) [31]. All drugs exhibit computational TPSA values between 40.62 and 115.38 $Å^2$ and have good intestinal absorption except drugs

Ceftriaxone, Clarithromycin, and Tetracycline (293.80 - 181.62 Å²). However, most of the drugs do not have adequate blood-brain barrier penetration, as the TPSA values are more than 60 Å², except Praziquantel (TPSA less than 40 Å²). The empirical conditions to satisfy Lipinski's rule and to manifest good oral bioavailability involve a balance between the solubility of a compound and its ability to diffuse passively through the different biological barriers. Compounds with high solubility are more easily metabolized and eliminated from the organism, thus leading to a lower probability of adverse effects and bioaccumulation. The solubility of Tetracycline is -1.83 which represents a good solubility index.

4. Conclusion

The main objective of this study is to computationally investigate the effective antibiotic drugs for COVID-19 treatment. Therefore, two conformations of Mpro are included in this study to examine the binding zones of antibiotic drugs. The docking result is suggesting S-3A (in native form) and S-1B (ligand-bound state) sites of Mpro are geometrically more preferred for accepting the most antibiotic drugs. Subsequently, one the bias of binding energy, the top three drugs are Clarithromycin (higher than -8.0 kcal/mol), Tetracycline (higher than -7.0 kcal/mol), and Praziquantel higher than -6.0 kcal/mol). However, the Clarithromycin and Tetracycline would not like to consider for further study because their intestinal absorption property is very poor (due to TPSA value are more than 140 Å²) and do not have adequate blood-brain barrier penetration potential (TPSA values are more than 60 Å²).

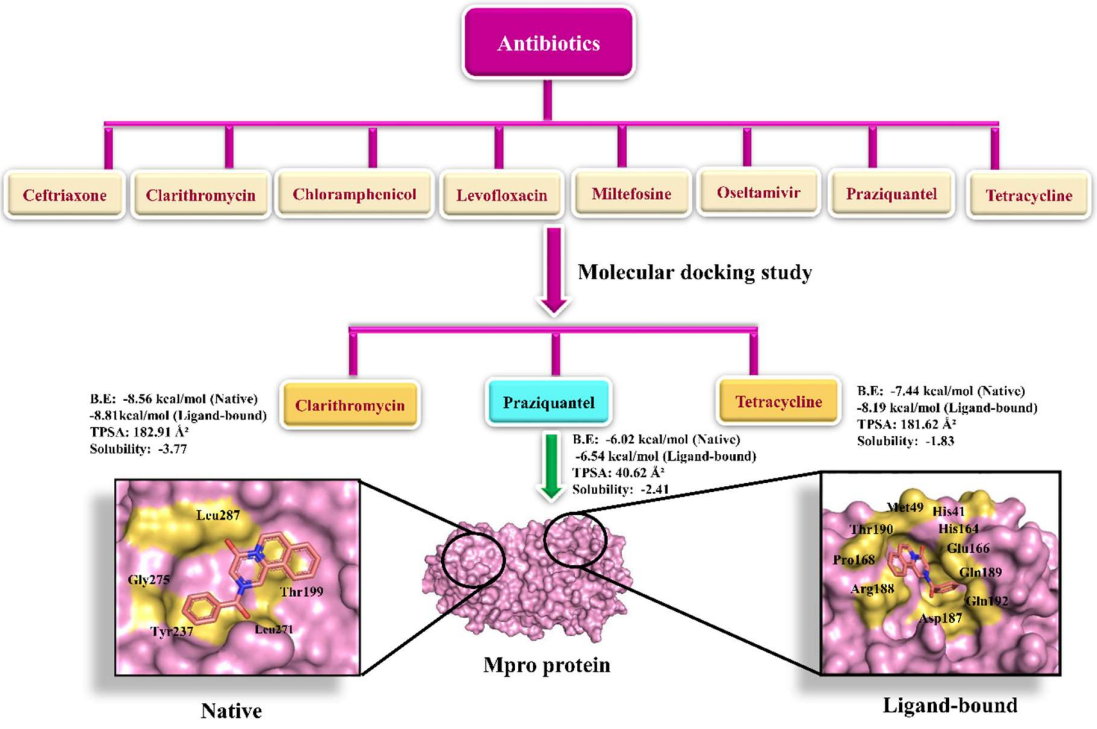

Figure 11: *Schematic representation of work. The eight antibiotic drugs were considered but Clarithromycin, Tetracycline, and Praziquantel were considered, and finally Praziquantel was suggested as its biological relevance with Mpro native and ligand bound state provide significance structural information with better biological acceptance.*

Therefore, Praziquantel is the only antibiotic drug that may consider for COVID disease because (i) its binding energy> 6.00kcal/mol in both the conformation of Mpro (ii) it is observed to bind in S-3A site in native conformation but S-1B in ligand bound state (nearby catalytic His41) (iii) its absorption property is very good, it has strong adequate blood-brain barrier penetration power, and its solubility is also better Figure 11. Hence, we proposed Praziquantel antibiotic drug will be the best option for future experimental and pre-clinical investigation for the possible treatment of nCOVID-19 disease.

Acknowledgement

We would like to convey our special thanks to the Department of Bioinformatics, Maulana Abul Kalam Azad University of Technology, W.B. for providing the computational facility and other institutional facility to conduct the research work.

References

1. Alimoradi Z, Lin CY, Pakpour AH. Worldwide estimation of parental acceptance of COVID-19 vaccine for their children: a systematic review and meta-analysis. Vaccines. 2023;11:533.

2. Kaynar M, Gomes AL, Sokolakis I, et al. Tip of the iceberg: erectile dysfunction and COVID-19. Int J Impot Res. 2022;34:152-7.

3. Thapa B, Pathak SB, Jha N, et al. Antibiotics use in hospitalised COVID-19 patients in a tertiary care centre: a descriptive cross-sectional study. J Nepal Med Assoc. 2022;60:625.

4. Adebisi YA, Jimoh ND, Ogunkola IO, et al. The use of antibiotics in COVID-19 management: a rapid review of national treatment guidelines in 10 African countries. Trop Med Health. 2021;49:1-5.

5. Chen N, Zhou M, Dong X, et al. Epidemiological and clinical characteristics of 99 cases of 2019 novel coronavirus pneumonia in Wuhan, China: a descriptive study. Lancet. 2020;395:507-13.

6. Molla MMA, Yeasmin M, Islam MK, et al. Antibiotic prescribing patterns at COVID-19 dedicated wards in Bangladesh: findings from a single center study. Infect Prev Pract. 2021;3:100134.

7. Zeshan B, Karobari MI, Afzal N, et al. The usage of antibiotics by COVID-19 patients with comorbidities: the risk of increased antimicrobial resistance. Antibiotics. 2021;11:35.

8. Goncalves Mendes Neto A, Lo KB, Wattoo A, et al. Bacterial infections and patterns of antibiotic use in patients with COVID-19. J Med Virol. 2021;93:1489-95.

9. Jin Z, Du X, Xu Y, et al. Structure of Mpro from SARS-CoV-2 and discovery of its inhibitors. Nature. 2020;582:289-93.

10. Tam NM, Nam PC, Quang DT, et al. Binding of inhibitors to the monomeric and dimeric SARS-CoV-2 Mpro. RSC Adv. 2021;11:2926-34.

11. Reyaz S, Tasneem A, Rai GP, et al. Investigation of structural analogs of hydroxychloroquine for SARS-CoV-2 main protease (Mpro): a computational drug discovery study. J Mol Graph Model. 2021;109:108021.

12. Bairagya HR, Tasneem A, Sarmadhikari D. Structural and thermodynamic properties of conserved water molecules in Mpro native: a combined approach by MD simulation and grid inhomogeneous solvation theory. Proteins. 2024.

13. Tasneem A, Rai GP, Reyaz S, et al. The possible molecular mechanism of SARS-CoV-2 Main Protease: new structural insights from computational methods. SciMed J. 2021;2:108-26.

14. Bairagya HR, Pal S, Gupta S. Investigation of structural analogues of azithromycin and remdesivir for SARS-CoV-2 Mpro: a computational approach in drug development. J Pharmacol Clin Toxicol. 2023;11:117.

15. Richards DM, Heel RC, Brogden RN, et al. Ceftriaxone: a review of its antibacterial activity, pharmacological properties and therapeutic use. Drugs. 1984;27:469-527.

16. Dowling PM. Chloramphenicol, thiamphenicol, and florfenicol. In: Giguère S, Prescott JF, Dowling PM (eds), Antimicrobial Therapy in Veterinary Medicine. (5thedn), John Wiley & Sons Inc., New Jersey, USA. 2013;pp.269-77.

17. Slay RM, Hewitt JA, Crumrine M. Determination of the postexposure prophylactic benefit of oral azithromycin and clarithromycin against inhalation anthrax in cynomolgus macaques. Clin Infect Dis. 2022;75:S411-6.

18. Hurst M, Lamb HM, Scott LJ, et al. Levofloxacin: an updated review of its use in the treatment of bacterial infections. Drugs. 2002;62:2127-67.

19. Haghani I, Yahyazadeh Z, Hedayati MT, et al. Antifungal activity of miltefosine against both azole-susceptible and-resistant *Aspergillus* strains. Int J Antimicrob Agents. 2023;61:106715.

20. Tan Q, Duan L, Ma Y, et al. Is oseltamivir suitable for fighting against COVID-19: *in silico* assessment, in vitro and retrospective study. Bioorg Chem. 2020;104:104257.

21. Summers S, Bhattacharyya T, Allan F, et al. A review of the genetic determinants of praziquantel resistance in *Schistosoma mansoni*: is praziquantel and intestinal schistosomiasis a perfect match? Front Trop Dis. 2022;3:933097.

22. Grossman TH. Tetracycline antibiotics and resistance. Cold Spring Harb Perspect Med. 2016;6:a025387.

23. Rose PW, Prlić A, Bi C, et al. The RCSB Protein Data Bank: views of structural biology for basic and applied research and education. Nucleic Acids Res. 2015;43:D345-56.

24. Wishart DS, Feunang YD, Guo AC, et al. DrugBank 5.0: a major update to the DrugBank database for 2018. Nucleic Acids Res. 2018;46:D1074-82.

25. Kalra S, Chauhan A. Identification of potent COVID-19 main protease (MPRO) inhibitors from flavonoids: an *in-silico* approach. J Ayurveda Holist Med. 2023;11:32-48.

26. Alghamdi HA, Attique SA, Yan W, et al. Repurposing the inhibitors of COVID-19 key proteins through molecular docking approach. Process Biochem. 2021;110:216-22.

27. Gyebi GA, Ogunyemi OM, Ibrahim IM, et al. SARS-CoV-2 host cell entry: an *in silico* investigation of potential inhibitory roles of terpenoids. J Genet Eng Biotechnol. 2021;19:1-22.

28. Jiang X, Kumar K, Hu X, et al. DOVIS 2.0: an efficient and easy to use parallel virtual screening tool based on AutoDock 4.0. Chem Cent J. 2008;2:1-7.

29. Fuhrmann J, Rurainski A, Lenhof HP, et al. A new Lamarckian genetic algorithm for flexible ligand-receptor docking. J Comput Chem. 2010;31:1911-8.

30. Bairagya HR, Pal S, Baral S. Identification of unique water molecules in human GRK2 protein with bound and unbound GβGγ subunit: a study by structural bioinformatics method. Int J Bioinfor Intell Comput. 2023;2:184-211.

Supporting Information

Table S1: *The Crystallographic structural parameters of the dimers of native-Mpro.*

Sl. No.	PDB ID	Resolution (Å)	R-Value Free/ R Value Work	Space Group	Chains/ Sequence Length	Refinement Method	Unit cell		Crystallographic parameters					No. of reflections
							Length (Å)	Angle (°)	PH	Solvent content	Mathews Coefficient	Mean isotropic b factor	Ratio (protein/water)	
01	7NTT	1.74	0.26/0.21	P 1 21 1	A/B/ 306	REFMAC	a =44.76 b =53.98 c=114.35	α=90 β=101.18 γ=90	NIL	38.6	2.00	29.06	17.06	52,172
02	7VJW	2.20	0.28/0.22	P 21 21 21	A/B/ 306	PHENIX	a =69.1 b =104.1 c =105.5	α=90 β=90 γ=90	8.5	56.98	2.86	56.08	73.68	39,287
03	7VJX	2.20	0.29/0.26	P 21 21 21	A/B/ 306	PHENIX	a=69.2 b =104.3 c =105.7	α=90 β =90 γ=90	8.5	57.21	2.87	62.04	47.86	39,396
04	7VK0	2.10	0.24/0.24	P 21 21 21	A/B/ 306	PHENIX	a=69.2 b =104.3 c =105.7	α=90 β=90 γ=90	8.5	57.21	2.87	58.40	44.63	45,326
05	7VK3	2.10	0.28/0.24	P 21 21 21	A/B/ 306	PHENIX	a=69.3 b =104.4 c =105.7	α=90 β=90 γ=90	8.5	57.31	2.88	53.55	40.72	42,380
06	7VK4	2.10	0.27/0.23	P 21 21 21	A/B/ 306	PHENIX	a=68.9 b =103.9 c =105.2	α=90 β =90 γ=90	8.5	56.86	2.85	64.73	659.71	44,742
07	7VK5	2.17	0.27/0.24	P 21 21 21	A/B/ 306	PHENIX	a=69.2 b =104.3 c =105.6	α=90 β=90 γ=90	8.5	57.17	2.87	57.49	58.76	41,092
08	7VK6	2.25	0.27/0.23	P 21 21 21	A/B/ 306	PHENIX	a=104.3 b =105.5 c =69.1	α=90 β =90 γ=90	8.5	57.06	2.86	60.36	45.07	36,768
09	7VK7	2.40	0.24/0.21	P 21 21 21	A/B/ 306	PHENIX	a=69.1 b =104.3 c =105.5	α=90 β=90 γ=90	8.5	57.06	2.86	77.57	76.10	30,465

Table S2: *The crystallographic structural parameters of the dimers of ligand-bound Mpro.*

Sl. No.	PDB ID	Resolution (Å)	R-Value Free/ R Value Work	Space Group	Chains / Sequence Length	Refinement Method	Unit cell		Crystallographic parameters					No. of reflections
							Length (Å)	Angle (°)	PH	Solvent content	Mathews Coefficient	Mean isotropic B factor	Ratio (protein/water)	
01	6Y2G	2.20	0.25/ 0.19	P 21 21 21	A/B/ 306	REFMAC	a=68.57 b=101.60 c=103.70	α=90 β=90 γ=90	8.5	53.92	2.67	40.89	14.92	37,448
02	7DGG	2.00	0.22/0.18	P 1 21 1	A/B/ 306	PHENIX	a=55.80 b =99.12 c =59.75	α=90 β=108.99 γ=90	6	46.75	2.31	26.85	13.35	37,990
03	7DGI	1.90	0.21/0.18	C 2 2 2 1	A/B/ 306	PHENIX	a=64.67 b =118.20 c =223.27	α=90 β=90 γ=90	6	61	3.15	26.66	7.28	67,801
04	7DK1	1.90	0.21/0.19	P 21 21 21	A/B/ 306	BUSTER	a=67.62 b =102.2 c =102.35	α=90 β=90 γ=90	6.5	53.4	2.64	39.17	10.78	56,431
05	7DPU	1.75	0.20/0.17	P 1 21 1	A/B/ 306	PHENIX	a=44.26 b =53.80 c =115.06	α=90 β=100.96 γ=90	NIL	38.13	1.99	23.83	11.35	52,603
06	7EN8	1.83	0.27/0.23	P 21 21 21	A/B/ 306	PHENIX	a=54.83 b =67.86 c =167.56	α=90 β=90 γ=90	4.6	46.61	2.3	15.61	8.67	55,655
07	7FAZ	2.10	0.24/0.19	P 21 21 21	A/B/ 306	PHENIX	a=67.61 b =97.96 c =101.59	α=90 β=90 γ=90	NIL	50.53	2.49	40.63	12.05	39929
08	7NT1	2.85	0.28/0.20	P 21 21 21	A/B/ 306	REFMAC	a =68.18 b =102.17 c =104.38	α=90 β =90 γ=90	6.5	54.29	2.69	56.79	87.13	17333
09	7NT2	2.15	0.25/0.20	P 21 21 21	A/B/ 306	REFMAC	a=68.16 b =100.59 c =104.73	α=90 β=90 γ=90	6.5	53.71	2.66	40.00	26.15	39220
10	7NT3	2.33	0.27/0.21	P 21 21 21	A/B/ 306	REFMAC	a=68.01 b =101.35	α=90 β=90	6.5	53.63	2.65	49.32	37.23	31556

							c =103.98	γ=90						
11	7NW2	2.10	0.22/0.19	P 21 21 21	A/B/306	BUSTER	a=67.45 b =99.75 c =103.61	α=90 β=90 γ=90	6.5	52.25	2.58	36.83	13.01	39471
12	7TLL	1.63	0.25/0.21	P 1 21 1	A/B/306	BUSTER	a=45.39 b =53.82 c =115.54	α=90 β=102.42 γ=90	NIL	39.54	2.03	27.23	14.21	53153
13	7U28	1.68	0.25/0.21	P 1 21 1	A/B/306	BUSTER	a=45.55 b =53.80 c =114.89	α=90 β=102.13 γ=90	NIL	39.48	2.03	23.93	14.86	46261
14	7U29	2.09	0.27/0.20	P 1 21 1	A/B/306	BUSTER	a=45.52 b =55.79 c =114.23	α=90 β=105.22 γ=90	NIL	40.49	2.07	30.31	23.58	28383
15	7VLP	1.50	0.22/0.20	P 1 21 1	A/B/305	PHENIX	a=55.48 b =98.70 c =59.42	α=90 β=108.72 γ=90	NIL	45.85	2.27	23.30	18.62	94010
16	7VLQ	1.94	0.23/0.20	P 21 21 21	A/B/300	PHENIX	a=67.85 b =102.02 c =103.27	α=90 β =90 γ=90	NIL	54.56	2.71	26.58	22.27	51406
17	7VTH	2.00	0.26/0.21	P 1 21 1	A/B/311	REFMAC	a=44.41 b =54.27 c =114.50	α=90 β =99.42 γ=90	NIL	37.79	1.98	18.55	20.34	34366
18	7VU6	1.80	0.28/ 0.22	P 1 21 1	A/B/308	REFMAC	a=55.47 b= 99.23 c=58.88	α=90 β=108.05 γ=90	NIL	45.76	2.27	17.80	12.88	52687
19	7VVT	2.51	0.25/0.23	P 21 21 21	A/B/306	PHENIX	a=67.99 b =30.12 c =103.18	α=90 β =90 γ=90	NIL	47.35	2.34	50.70	77.75	22010
20	7WYP	2.30	0.27/0.22	P 21 21 21	A/B/306	PHENIX	a=67.81 b =101.28 c =103.15	α=90 β=90 γ=90	7.5	53.01	2.62	55.30	57.09	32303
21	7XAR	1.60	0.21/0.17	P 1 21 1	A/B/306	REFMAC	a=47.03 b =63.36 c =102.83	α=90 β=90.40 γ=90	NIL	45.68	2.26	22.40	10.01	76114